Numerical Modelling of Biogeochemical Regime Response to Decadal Atmospheric Variability During 1960–2000 in the Black Sea

Yunchang He, Emil Stanev, Evgeniy Yakushev, and Joanna Staneva

Abstract Based on an analysis of observations and one-dimensional coupled hydrophysical biogeochemical model, long-term variability of the physical and biogeochemical structure of oxic and suboxic layers in the Black Sea is studied here. The correlation between large-scale atmospheric forcing [2 m air temperature, surface level pressure, surface wind and North Atlantic oscillation (NAO) index] and local responses is the main point. The comparison of model performance with respect to spatial and temporal distribution of biogeochemical variables against observed vertical distribution patterns is quite good. It is demonstrated that during 1960–2000, the long-term variability of winter-mean-simulated SST in the Black Sea is reasonably well correlated with the variability of 2 m air temperature. Furthermore, it is demonstrated that the thermal state of the upper ocean impacts largely the variability of concentration of biogeochemical variables, such as oxygen and nitrate. The teleconnection between NAO and Black Sea biogeochemistry manifests differently for the periods 1960–2000. The corresponding regime shifts are also associated in a vital way with the large-scale forcing.

Keywords Atmospheric forcing, Biogeochemical model, Black Sea, Decadal variability, Oxygen

Contents

Y. He (✉), E. Stanev, and J. Staneva
Helmholtz-Zentrum Geesthacht, Geesthacht 21502, Germany
e-mail: yunchang.he@hzg.de

E. Yakushev
Norwegian Institute for Water Research, Gaustadalleen 21, NO-0349 Oslo, Norway

E.V. Yakushev (ed.), *Chemical Structure of Pelagic Redox Interfaces: Observation and Modeling*, Hdb Env Chem (2013) 22: 253–272, DOI 10.1007/698_2011_103,

Abbreviations

AT	Air temperature
CIL	Cold intermediate layer
DPT	Dew point temperature
GOTM	General Ocean Turbulent Model
NAO	North Atlantic oscillations
OM	Organic matter
ROLM	Redox-Layer Model
SST	Sea surface temperature

1 Introduction

Permanent anoxic conditions are observed in lakes, fjords and ocean basins such as Black Sea, Baltic Sea and Cariaco Trench, which are characterized by extremely stable stratification. In the Black Sea, the biogeochemical system adjusted to the physical stratification in an unique way, building thus the largest anoxic environment in the world. Major changes of biogeochemical variables are observed across levels of constant density, while gradients along density are extremely small [1–3]. A typical vertical profiles observed in the centre of the Black Sea are shown in Fig. 1. Oxygen is almost at atmospheric saturation in the upper layer (0–40 m) and drops sharply below the detection limit of 3 μM at about the depth of 60 m. The first appearance of the hydrogen sulphide occurs at about 80 m and then increased continuously to more than 40 μM of about 150 m. The nitrate maximum appears at about 60 m, and the ammonia starts to increase at about 75 m several metres above the sulphidic boundary. The same profiles are shown versus density in the figure on the right (Fig. 1). It is noteworthy that biogeochemical structure of the water column is characterized by no-overlap of dissolved oxygen and hydrogen sulphide layers. The corresponding layer is known as the suboxic layer (the zone without oxygen and hydrogen sulphide, [4]). Yakushev et al. [5] numerically proved with the model that the manganese cycle in the Black Sea could explain this layering.

The present-day vertical structure is very stable and has been established as a consequence of the re-connection between the Black Sea and the Mediterranean. Some analyses of long-term variations of chemical [6] and ecological [7, 8] systems in the Black Sea identify regime shifts, which could be due to either anthropogenic or climatic forcing.

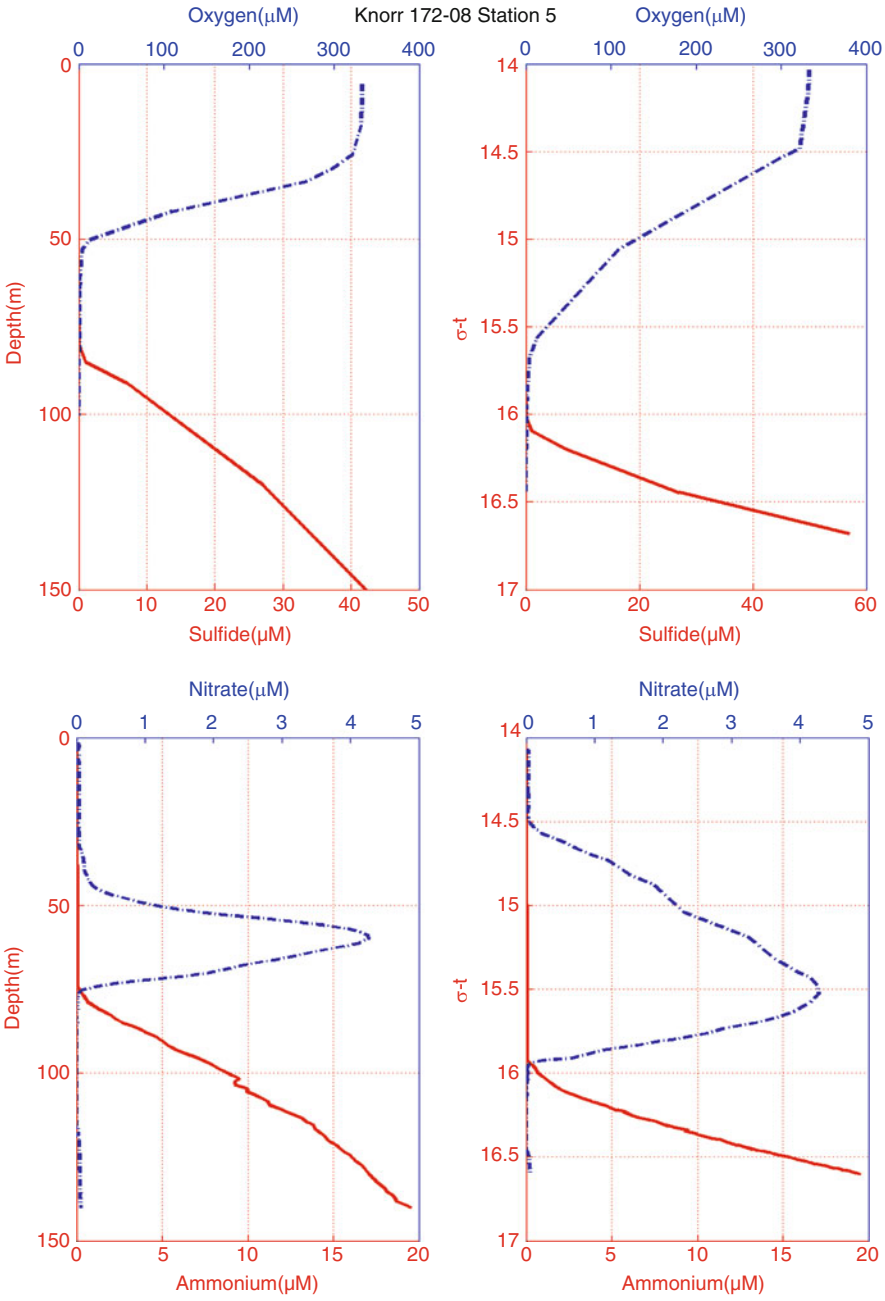

Fig. 1 Vertical profiles of basic chemical end ecological variables in the Black Sea (*Leg* 8, *Stn* 5); *top*: oxygen/sulphide data in situ; *bottom*: nitrate/nitrite/ammonia pump cast data, during R/V Knorr Cruise 2003: The Black Sea; for more details, see: http://www.ocean.washington.edu/cruises/Knorr2003/data/Vol_Oxygen_Sulfide/08-5.html

The motivation for this study is to test the capability of a complex biogeochemical model to reproduce interannual variability triggered by the atmosphere. In this chapter, we use a 1D model, a first step that is necessary to understand the possible reaction of natural water systems to atmospheric forcing. Testing performance of 1D biogeochemical model and validation against observations will also be illustrated here. Major interest is on the upper layer variability. The chapter is structured as follows. We first describe the numerical model and sensitivity experiments carried out, which is followed by a discussion of results and short conclusions.

2 Model and Materials

2.1 Description of the Model

The biogeochemical model used in this study is Redox-Layer Model (ROLM, [5]). This model includes production and decay of organic matter (OM), and reduction and oxidation of nitrogen, sulphur, manganese and iron. The following compartments are included (Fig. 2): dissolved oxygen (O_2), hydrogen sulphide (H_2S), total

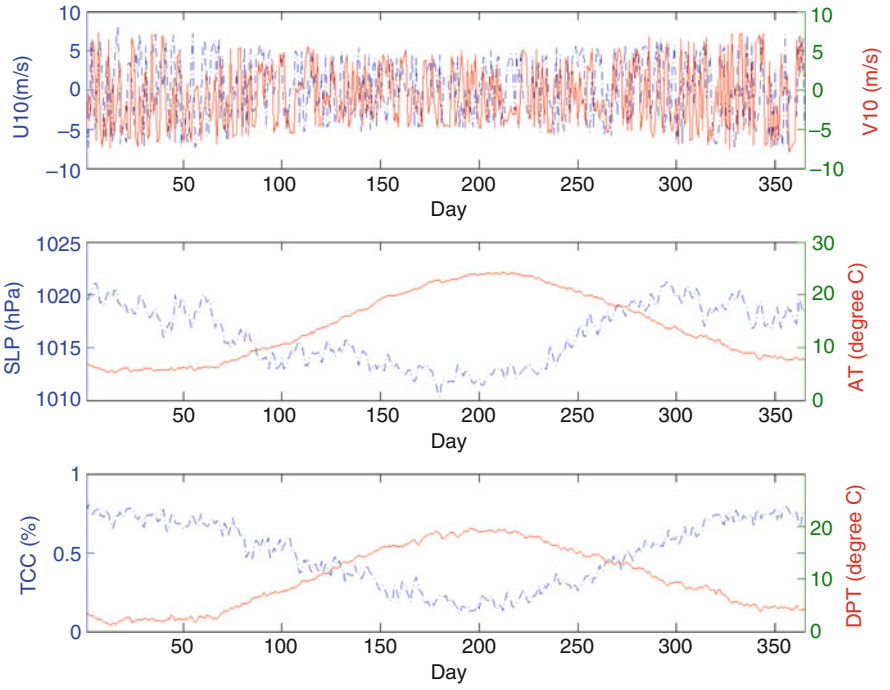

Fig. 2 Forty-five-year mean value for meteorological forcing data of wind speed, sea level pressure, air temperature, dew point temperature and total cloud cover

elemental sulphur (S_0), thiosulphate (S_2O_3), sulphate (SO_4), ammonia (NH_4), nitrite (NO_2), nitrate (NO_3), particulate organic nitrogen (PON), dissolved organic nitrogen (DON), phosphate (PO_4), particulate organic phosphorus (POP), dissolved organic phosphorus (DOP), bivalent manganese (Mn_2), trivalent manganese (Mn_3), quadrivalent manganese (Mn_4), bivalent iron (Fe_2), trivalent iron (Fe_3), phytoplankton (Phy), zooplankton (Zoo), aerobic heterotrophic bacteria (Bhe), aerobic autotrophic bacteria (Bae), anaerobic heterotrophic bacteria (Bha) and anaerobic autotrophic bacteria (Baa). ROLM was chosen for the multi-decadal calculations because this model describes losses of oxygen for both mineralization of organic matter and oxidation of the reduced forms of sulphur, nitrogen, manganese and iron. ROLM considers also the transformation of nitrogen from reduced to oxidized forms (i.e. between NO_3, NO_2 and NH_4). Unlike the other existing models for the Black Sea [9, 10], organic mater production due to photosynthesis and chemosynthesis is parameterized, and thus feedbacks between the upward fluxes of nutrients and organic mater production are accounted for. A detailed description of the model is presented by Yakushev [5].

The model is coupled online with the General Ocean Turbulent Model (GOTM, [11]). This is a one-dimensional water column model for the most important hydrodynamic and thermodynamic processes related to vertical mixing. The basic set of equations (1–7) for temperature T, salinity S, mean horizontal velocity components u and v, pressure P, turbulent kinetic energy (TKE) k and the TKE dissipation rate ε are:

$$\frac{\partial T}{\partial t} = \frac{\partial}{\partial z}\left((\upsilon'_t + \upsilon')\frac{\partial T}{\partial z} \right) - \gamma^T (T - T_o), \tag{1}$$

$$\frac{\partial S}{\partial t} = \frac{\partial}{\partial z}\left((\upsilon'_t + \upsilon')\frac{\partial S}{\partial z} \right) - \gamma^S (S - S_o), \tag{2}$$

$$\frac{\partial u}{\partial t} = \frac{\partial}{\partial z}\left((\upsilon_t + \upsilon)\frac{\partial u}{\partial z} \right) + fv, \tag{3}$$

$$\frac{\partial v}{\partial t} = \frac{\partial}{\partial z}\left((\upsilon_t + \upsilon)\frac{\partial v}{\partial z} \right) - fu, \tag{4}$$

$$\frac{\partial P}{\partial z} = -g\rho, \tag{5}$$

$$\frac{\partial k}{\partial t} = \upsilon_k \frac{\partial^2 k}{\partial z^2} + P + B - \varepsilon, \tag{6}$$

$$\frac{\partial \varepsilon}{\partial t} = \upsilon_\varepsilon \frac{\partial^2 \varepsilon}{\partial z^2} + \frac{\varepsilon}{k}(c_{\varepsilon 1} P + c_{\varepsilon 3} B - c_{\varepsilon 2}\varepsilon), \tag{7}$$

where υ'_t and υ' are molecular and turbulent diffusivity of temperature and salinity, υ and υ_t are molecular and turbulent viscosity (momentum), f is the Coriolis parameter, and υ_ε and υ_k are the turbulent diffusivities of energy dissipation and TKE, respectively. Relaxation with the time scale $1/\gamma^{(T,\ S)}$ towards prescribed profiles (T, S) is enabled in deep layers to compensate for the missing fluxes in one-dimensional model.

The shear stress production P and the buoyancy production B are:

$$P = \upsilon_t \left(\left(\frac{\partial u}{\partial z} \right)^2 + \left(\frac{\partial v}{\partial z} \right)^2 \right), \tag{8}$$

$$B = -\upsilon'_t N^2, \tag{9}$$

where

$N^2 = \dfrac{-g}{\rho_0} \dfrac{\partial \rho}{\partial z}$ is the Brunt–Väisälä frequency.

The turbulent viscosity and diffusivity can be calculated using the relation of Kolmogorov and Prandtl:

$$\upsilon_t = c_\mu \frac{k^2}{\varepsilon}, \quad \upsilon'_t = c'_\mu \frac{k^2}{\varepsilon}. \tag{10}$$

The turbulent diffusivities for k and ε are:

$$\upsilon_k = \frac{c_\mu}{\sigma_k} \frac{k^2}{\varepsilon}, \quad \upsilon_\varepsilon = \frac{c_\mu}{\sigma_\varepsilon} \frac{k^2}{\varepsilon}. \tag{11}$$

All parameters in the above formula are listed in Table 1 [11, 12]. The surface fluxes is calculated by means of bulk formulae which was developed by Kondo [13]. Meteological forcing and dew point temperature are specified, while the solar radiation is not prescribed.

The physical model is coupled to and solves one-dimensional vertical diffusion equations for 24 non-conservative substances of the type:

$$\frac{\partial C_i}{\partial t} = \frac{\partial}{\partial z} \left((\upsilon'_t + \upsilon) \frac{\partial C_i}{\partial z} \right) - \frac{\partial}{\partial z} \left((W_C + W_M) \times C_i \right) + R_{C_i}, \tag{12}$$

Table 1 Parameters of the K-ε model [26]

Model constant	Value	Definition
$c_{\varepsilon 1}$	1.44	Empirical coefficient of dissipation equation
$C_{\varepsilon 2}$	1.92	Empirical coefficient of dissipation equation
$c_{\varepsilon 3}$ ($B < 0$)	−0.4	Empirical coefficient of dissipation equation for stable stratification
$c_{\varepsilon 3}$ ($B > 0$)	1	Empirical coefficient of dissipation equation for unstable stratification
σ_ε	1.3	Schmidt number for TKE diffusivity
σ_k	1	Schmidt number for TKE diffusivity

where C_i is the concentration of a model variable, W_C the sinking velocity of particulate matter; W_{Me} accounts for the contribution of settling of Mn hydroxides, and R_{C_i} describes biogeochemical production or consumption. These terms given by Yakushev [5] were used in the present study parameter values. Meanwhile, some parameters about phytoplankton on specific growth, respiration, mortality and excretion rate changed a little according to other literatures to make the model results more closer to the real situation.

2.2 Analysis of Forcing and Initial Data

2.2.1 Forcing Data

Forcing data for the physical model consists of radiation (including clouds), 10 m wind speed, 2 m air temperature and dew point temperature, as well as sea level pressure. They are produced by the European Centre for Medium-Range Weather Forecasts (ECMWF) and were kindly made available for the period 1958–2002 in the frame of Southern European Seas: Assessing and Modelling Ecosystem changes (SESAME) project by the INGV, Italy. The temporal sampling rate is 6 h. The data have spatial resolution of 0.25°. From these data, we extract forcing corresponding to an open sea location (32.625°E, 43.177°N). Atmospheric variability is characterized by a pronounced seasonal cycle, which is exemplified in Fig. 2 by the mean year for the 45-year model integration period. In the study, all the atmospheric forcing data are calculated in winter-mean (December–February).

The Black Sea regime shifts appear to be sporadic events forced by the strong transient decadal perturbations, and therefore differ from the multi-decadal scale cyclical events observed in pelagic ocean ecosystems under low-frequency climatic forcing [14]. The North Atlantic oscillation (NAO) index is known to be the most prominent mode of low-frequency variability controlling atmospheric circulation and climate over the North Atlantic and Eurasia [15]. The positive winter NAO index is associated with stronger north-south pressure gradient, more cold and dry air conditions in the Mediterranean and Black Sea region, and more moisture and heat transported in Scandinavian area. Conversely, the negative NAO index supports warmer air temperatures in the southern Europe. The NAO index for the period 1960–2000, defined as the normalized sea level pressure difference measured in meteorological stations located at Gibraltar and Iceland [16], was obtained from the Climate Prediction Centre of National Weather Service in NOAA (http://www.cpc.noaa.gov/products/precip/CWlink/pna/nao_index.html). Monthly values were averaged for winter season (December–February).

2.2.2 Initial Conditions

Initial conditions correspond to the annual mean temperature and salinity profiles for the interior part of the basin. Because the model is one-dimensional (no horizontal fluxes are computed or prescribed), we relax temperature and salinity below the depth of CIL to climatology. At every time step, temperature and salinity profiles used for relaxation are interpolated to the actual GOTM model grid. This procedure ensures that the simulations remain consistent with the dominating stratification in deep layers. At the same time, upper layer characteristics are free to adjust to surface forcing.

At the sea surface, all chemical and ecological constituents were set to zero except for O_2, NO_3 and PO_4 that were parameterized as follows [5]. At the lower boundary, which is at the depth of 200 m, constant values were specified: NH_4 = 20 μM, H_2S = 60 μM, MnII = 8 μM, FeII = 0.4 μM, PO_4 = 4.5 μM, which corresponds to existing observations.

2.3 Numerical Experiments

We define two scenarios, which we run for 45 years each with data described above. The difference between them is that in the first one called Scenario (I) we use the full atmospheric signal, which contains interannual (I) variability. In second scenario, we substitute the atmospheric forcing by the mean year, which is perpetually repeated for 45 times; therefore, the name of this scenario is perpetual (P).

In view of the simple conditions of the 1D physical biochemical model, the meteorological forcing was the only driving source. Four sensitivity experiments in 1-year run on air temperature, dew point temperature, wind and sea level pressure were designed to test the main affecting factors. On the basis of the scenario P, we designed six sensitivity experiments on AT, DPT, wind and SLP independently. The first sensitivity experiment run by increasing 2° on AT value, and the other meteorological forcing kept unchanged. The second sensitivity experiment run by decreasing 2° on AT value, and the others parameters kept unchanged. The similar experiments run with increasing and decreasing 2° on DPT, increasing and decreasing 1 m s^{-1} on wind, and increasing and decreasing 7 Pa on SLP independently. All the sensitivity experiments run 2 years, as well as the reference run without any change in meteorological forcing.

For oxygen distribution at CIL (between 50 and 75 m) in sensitivity experiments (Fig. 3), air temperature with reduction of 2° caused oxygen concentration go up to nearly 9 μM, from 30 μM at reference to 40 μM. On the contrary, air temperature increasing 2° made oxygen concentration go down around 10 μM all the year. The dew point temperature increased 2°, the oxygen concentration decreased to the maximum of 3 μM in summer when compared to that of reference, and vice versa. The wind either increased or decreased 1 m s^{-1}, and oxygen concentration at CIL

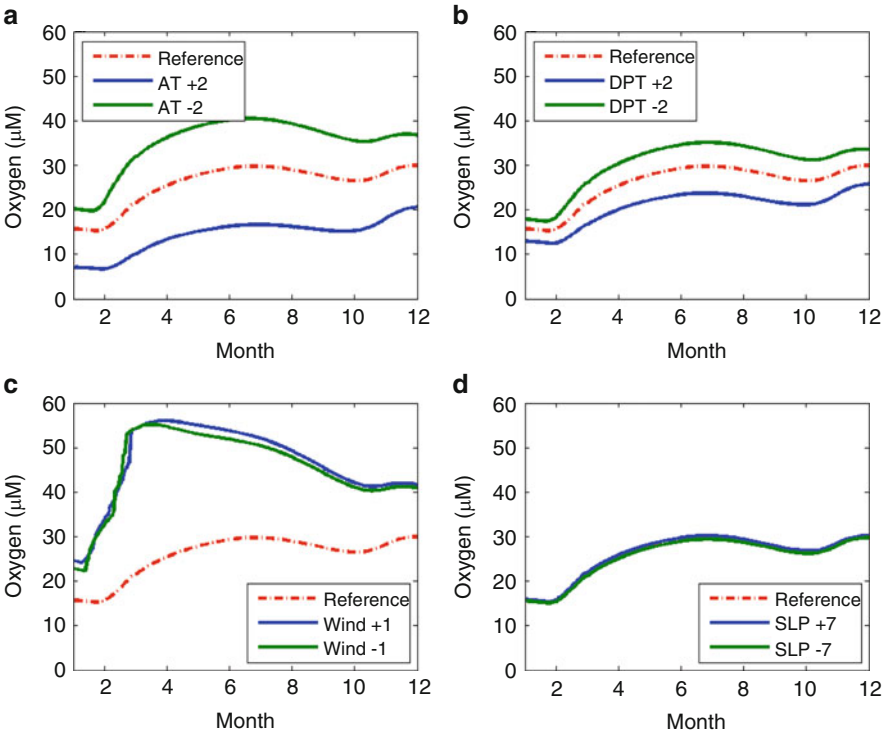

Fig. 3 Oxygen variations at CIL (50–75 m) in the different sensitivity experiments [(**a**) air temperature; (**b**) dew point temperature; (**c**) wind; (**d**) sea level pressure]. The oxygen concentration from perpetual scenario was the reference (*red dash line*)

goes up, especially in spring bloom. The change in sea level pressure had negligible effect on oxygen concentration at CIL. From the analysis and comparison, the effect on oxygen at CIL among all meteorological forcing in the sensitivity experiments, the changes in wind and air temperature, should be the more important factors, and then the dew point temperature was less important affecting factors on variability of oxygen at suboxic zone. For nitrate concentration experiments at the same layer (Fig. 4), the variability of air temperature and dew point temperature brought obvious change, and the decrease of 2° in air temperature caused nitrate concentration going up 1 μM. On the contrary, the increase of 2° in air temperature caused nitrate concentration going down 2 μM. The change in dew point temperature had a similar effect on nitrate, while the influence was less to half. Whether wind increased 1 m s^{-1} or decreased 1 m s^{-1}, the concentration of nitrate went up less than 1 μM. The variability of 7 Pa on sea level pressure caused very weak influence on nitrate concentration.

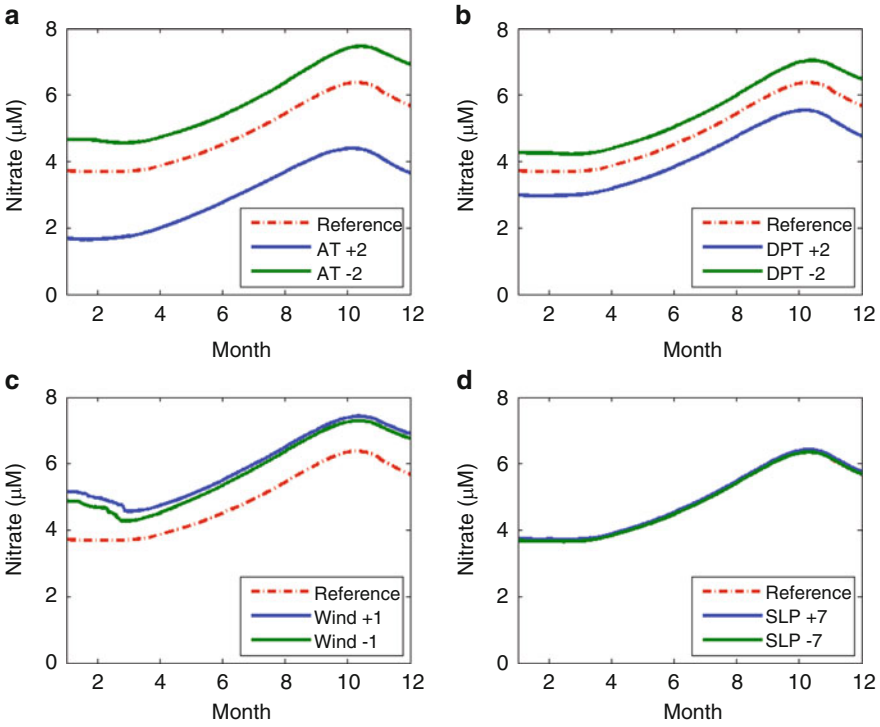

Fig. 4 Nitrate variations at CIL (50–75 m) in the different sensitivity experiments [(**a**) air temperature; (**b**) dew point temperature; (**c**) wind; (**d**) sea level pressure]. The nitrate concentration from perpetual scenario was the reference (*red dash line*)

2.4 Model Validations

The performance of the model is illustrated below by validating the simulations against observations from the Knorr Black Sea Cruise in the centre of the Black Sea Western Gyre in 2003. Because the processes in the Black Sea align to isopycnals, we present simulated profiles against depth and density separately. Figure 5 reveals the typical vertical distribution of temperature, salinity, oxygen and hydrogen sulphide. Overall, the comparison is quite good; however, some differences are to be mentioned: the cold intermediate layer (CIL) in the model is a little more diffuse than in the observations, and the oxygenated water penetrates slightly deeper in the upper layer. As a success of the simulation, one could mention the approximate agreement of the isopycnic depth of the suboxic layer (a layer characterized by the absence of dissolved oxygen and hydrogen sulphide; Murray et al. [4]) in the observations and simulations.

Here, we will describe the model performance at the depths above and around the depth interval where suboxic layer is usually observed (Fig. 6). In the numerical simulations, position of suboxic zone is at the density layer of 15.2–15.7 kg m^{-3}.

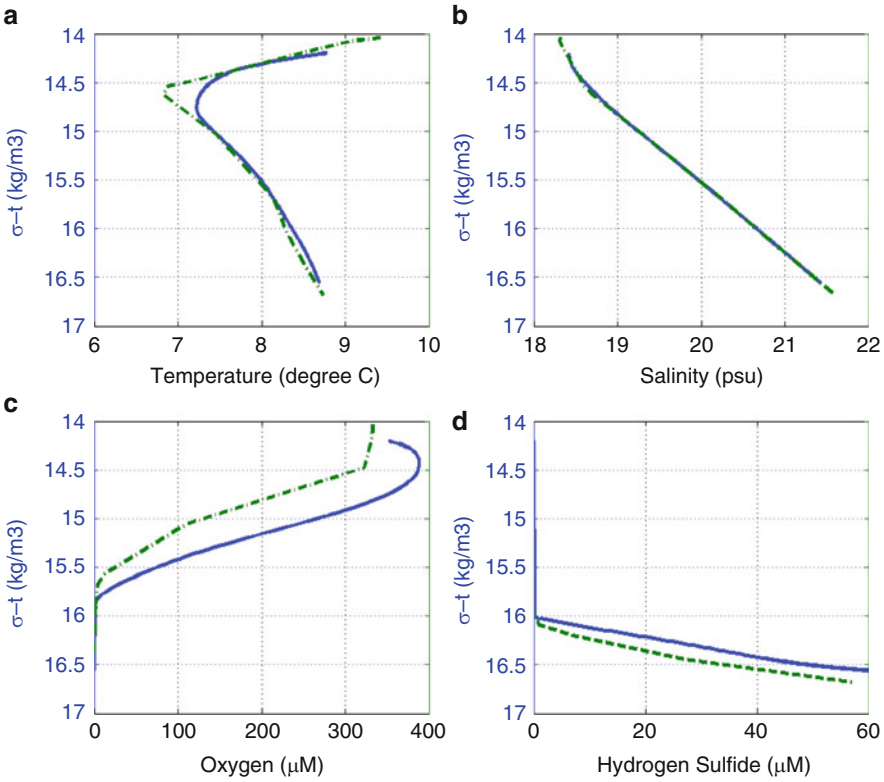

Fig. 5 Comparisons of vertical distribution of temperature, salinity, oxygen and hydrogen sulphide between simulation and observation versus depth and density. Observations used for intercomparisons are taken from Knorr Cruise in 2003

Large variations were observed in the distributions of oxygen in surface layers mostly due to temperature change. Maximum of oxygen of about 380 μM occurred at sea surface, which was similar to the observed data [8]. The profile reached zero concentration (less than 0.5 μM) at σ_θ 15.2 kg m^{-3}, which was little thinner than in the observed data (15.3–16.0 kg m^{-3}) [17]. Vertical distribution of nitrogen compounds (NH_4, NO_2, NO_3) showed that onset of NH_4 appears at about σ_θ 15.4 kg m^{-3}, and the maximum of NO_2 appeared at the depth where the concentrations of NH_4 and NO_3 were equal. The onset of Mn_2 increased greatly where the onset of H_2S occurred. The vertical distribution of H_2S was similar in summer and winter. The maximum of NO_3 appeared approximately at the depth where the O_2 dropped below 10 μM.

The depth of redox layer was 65 and 90 m, correspondingly. In the model, the oxidation of Mn_2 resulted in the formation of alternative electron acceptors, which had a sinking rate to accelerate the downward transport. O_2 dropped to 0 at the same depth where Mn_2 onset appeared that was same as in the observations [5].

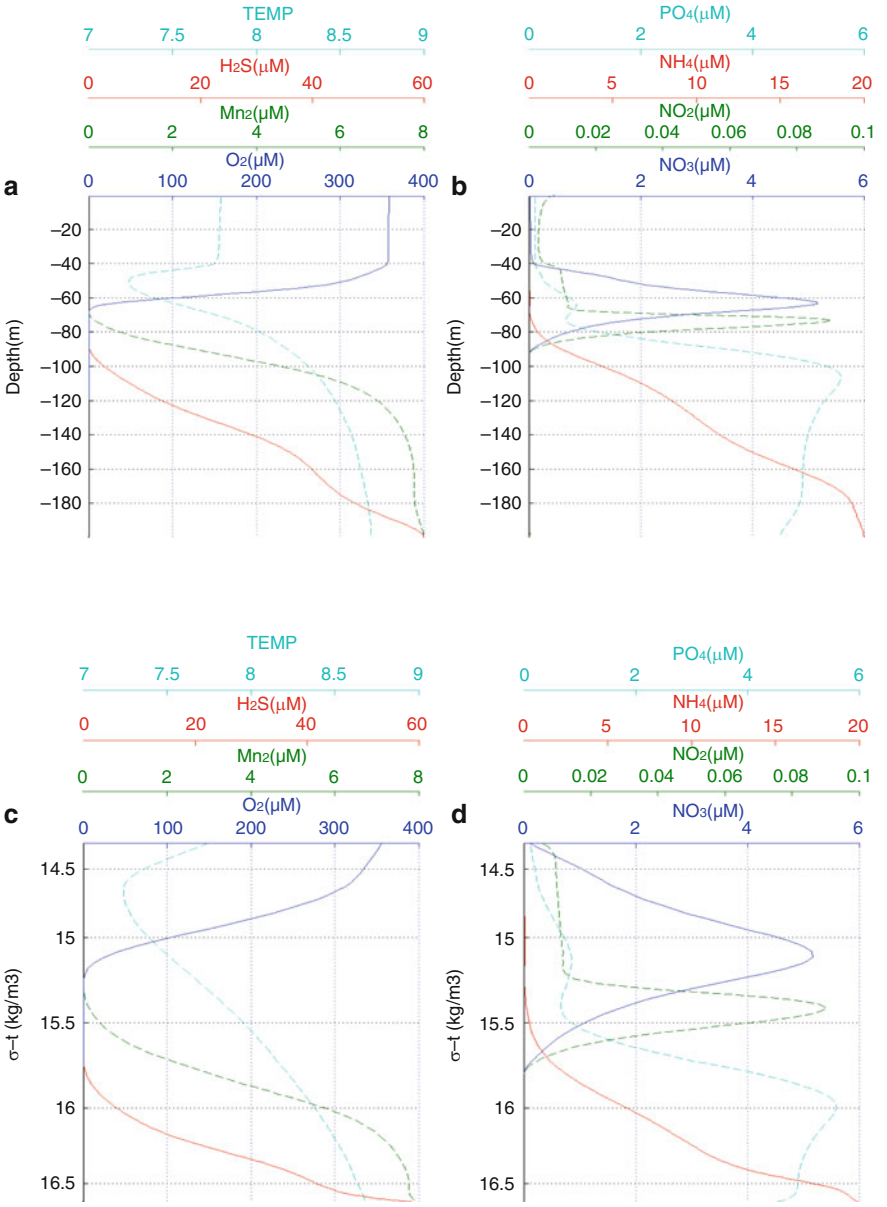

Fig. 6 Winter-mean (December–February) vertical distribution of the main chemical variables versus depth (**a**, **b**) and versus density (**c**, **d**) in 1960

Furthermore, Yakushev and Debolskaya [18] suggested that the reduction of Mn_4 by H_2S was very intensive, and the reaction can be balanced by the flux from below. Hence, we may conclude that the main biogeochemical features of

the redox layer in the central Black Sea known from observations are well reproduced by the 1D model.

3 Interannual Variability of Simulated Biogeochemistry Responses

Decadal and interannual variability in atmospheric state, in particular in the European region, is well pronounced when analysing data for winter months. Interannual variability in the physical system has been analysed by Stanev et al. [3, 19] and Tsimplis et al. [20]. One important result from the above studies is that the deep layers of the Black Sea do not show pronounced sensitivity to interannual variations in forcing. This is due to the strong stratification decoupling surface and deep layers. However, as it has been demonstrated by Staneva et al. [21], responses in the upper layers and down to the depth of CIL are very clear. Recently, the response of a number of biogeochemical parameters to long-term atmospheric variability has been addressed by Oguz [22].

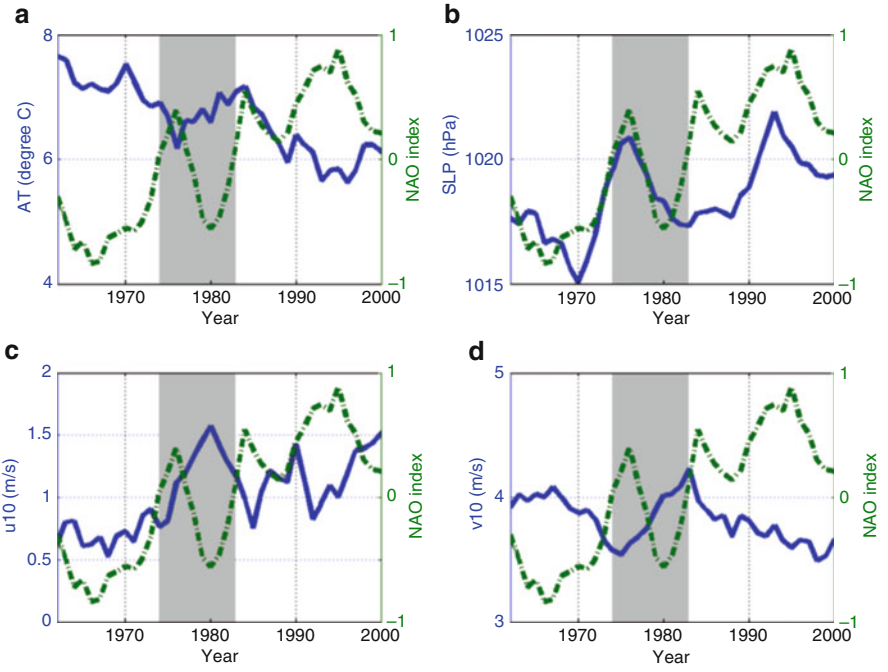

Fig. 7 Interannual variability of air temperature (**a**), SLP (**b**) and wind components u10 (**c**) and v10 (**d**) in winter (December–February) compared with the winter NAO index. Data were 5-year moving averaged

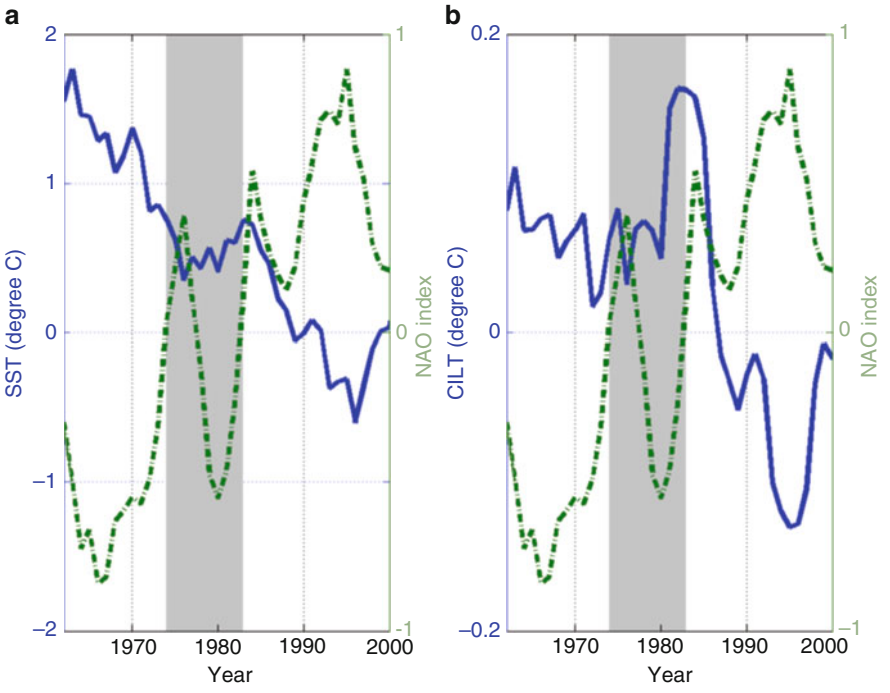

Fig. 8 Interannual variability of simulated annual SST (**a**) and CIL temperature (**b**) anomalies in winter (December–February) compared with the winter NAO index. Data were 5-year moving averaged

There is a consensus that during periods of positive winter NAO index, cold and dry air intrusions into the Black Sea region dominate. Conversely, during times of negative NAO index, warmer air temperatures dominate the Black Sea region. Figures 7 and 8 showed the comparison between winter NAO index and air temperature, sea level pressure, wind, SST anomaly and CIL temperature anomaly in winter during 1962–2000. All the data were 5-year moving averaged. Clearly, there were three peaks of the winter NAO index in 1976, 1984 and 1995, separately. From 1960s to 1973, the negative winter NAO index dominates; the air temperature had a decreasing trend, also with SST, CIL temperature and dew point temperature. The following 9 years between 1974 and 1982, the winter NAO index changed from positive to negative, also in turn, frequently. At the same time, the air temperature increased a little about 1°, and the same trends appeared for SST, CIL temperature and dew point temperature. At the third period in 1983–1995, positive winter NAO index took the main role, and the air temperature, SST, CIL temperature and dew point temperature also decreased. After 1995, all the situations varied again. From the wind components in winter time, the southwest wind prevailed the four decades from 1960s to 1990s in the observation station. It was similar to the observation statistics wind data [23], and an occurrence of the SW wind regime (61%) is approximately two times as much as of the NE regime (28%) during the

period 1950–2004 in the Black Sea. The interannual variability in the Black Sea diagnosed from GOTM does not reveal a very clear correlation between analysed variables and NAO index, in particular when shorter periods are concerned. As explained by Oguz [22], NAO is not the only one relevant for the region climatic index; therefore, perfect correlation is not to be expected.

Summarizing the above results, we remind that the trend variabilities of air temperature, dew point temperature, SST and CIL temperature show some correlation with winter NAO index. This could indicate that shifts in the response pattern of physical variables of the Black Sea are possible.

Long-term variations in the structure of thermohaline had been discussed by many scientists. According to Belokopitov [24], extreme cold winters occurred in 1964, 1972, 1976, 1985 and 1993.

A two-layer structure can be distinguished in the vertical distribution of oxygen in the Black Sea (Fig. 1). A 90–110% saturated with oxygen upper layer is at or above atmospheric solubility due to gas exchange and biological production. It shows significant seasonal variations, and the concentrations there vary from 300–370 μM in February–April to 200–250 μM in July–August depending on the seasonality of temperature-influenced air–water exchange and OM production and decomposition [8]. In the lower layer, the oxygen concentrations decrease. A layer of decreasing oxygen concentration (oxycline) coincides with the main pycnocline (halocline). Oxygen decreases quasi-linearly with depth from 250–300 μM above the main pycnocline to 10–20 μM at the density level of σ_θ 15.50–15.60 kg m^{-3}. The vertical gradient of oxygen in this layer is 7–10 μM m^{-1}. Below this depth, the vertical gradient of oxygen decreases significantly to 0.5–1.5 μM m^{-1}. Around the densities of σ_θ, 15.90–16.00 kg m^{-3} dissolved oxygen decreases to below detection [8].

A supply of oxygen from the upper layer to the lower one depends on an intensity of the vertical mixing. In case of the presence of a strong thermohaline structure, oxygen is consumed faster than it can be replaced by vertical and lateral fluxes at a depth of CIL, about 70 m. But after a cold winter, the vertical mixing intensifies and the oxygen concentrations increase. Such an increase in mixing should also affect supply of nutrients (i.e. nitrate) to the surface layer and therefore its potential biological productivity. This means that the yearly variability of oxygen, phytoplankton and nitrate concentrations at both surface and CIL may have also certain correlations with winter NAO index.

According to the model simulations (Fig. 9), the NAO index in winter influences the anomalies of oxygen, phytoplankton and nitrate concentrations at both surface and CIL. The oxygen concentration at the surface (Fig. 9a) had same trend of increasing with NAO in 1962–2000 that is opposite to temperature (Fig. 7a). Before 1990, the oxygen anomaly kept negative and became positive in the most time of 1990s, when it might be caused by high solubility of oxygen due to the colder SST. From the middle 1970s to middle 1980s, oxygen maintained relatively stable, while phytoplankton and nitrate appeared maximum. Furthermore, the correlation of general trend between winter NAO and phytoplankton and nitrate in surface layers was clearly negative. Noteworthy is that the correlation between above

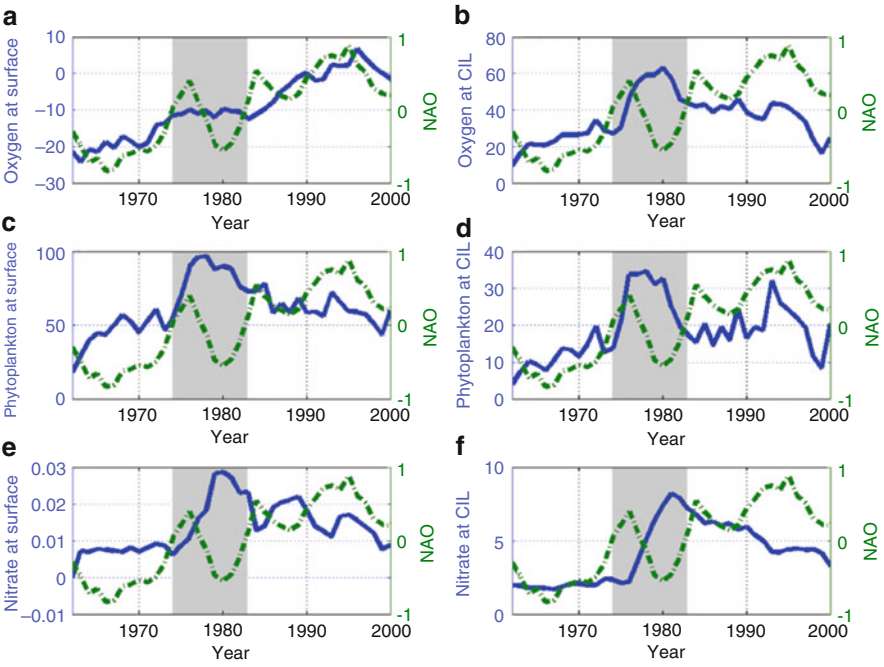

Fig. 9 Interannual variability in anomalies of oxygen, phytoplankton and nitrate concentrations in winter time simulated at sea surface (0–5 m) (*left*) and CIL (60–90 m) (*right*) versus winter NAO index (December–February). (**a**) Oxygen at surface versus winter NAO index; (**b**) oxygen at CIL versus winter NAO index; (**c**) phytoplankton at surface versus winter NAO index; (**d**) phytoplankton at CIL versus winter NAO index; (**e**) nitrate at surface versus winter NAO index; (**f**) nitrate at CIL versus winter NAO index

phytoplankton and nitrate in the surface layer is much stronger than oxygen, which may reflect that at surface phytoplankton concentration depends on nitrate, while the surface layer oxygen can be affected by other factors, i.e. temperature-forced changes in the air–water exchange (Figs. 5a and 7a).

Meanwhile, an interannual variability of oxygen at CIL correlate better with an interannual variability of phytoplankton and nitrate both in the CIL and at the surface (Fig. 9b–f). An increase in oxygen concentrations at CIL depends on the intensity of mixing as well as an increase in nitrate and phytoplankton. It was notable that nitrate was preserved stable in 1960s and in the first half of 1970s at surface and at CIL. Both surface and CIL phytoplankton and nitrate concentrations and oxygen at CIL increased very rapidly in the late half of 1970s, when the winter NAO shifted very intensively. Consistent with the above analysis, one comes to the conclusion that the winter NAO can be regarded as a potential long-term forcing explaining the decadal variability of biogeochemical process.

4 Discussion and Conclusions

We demonstrated in this chapter that the coupled numerical model simulations reveal a pronounced interannual variability of state variables in the Black Sea, allowing to conclude that changes in NAO during the past 40 years could be considered as important driver for changes in the Black Sea biogeochemistry. Both at surface layer and at CIL layer, the concentrations of oxygen, nitrate and phytoplankton directly or indirectly respond to the long-term winter NAO index. The basic points of our findings may be briefly summarized as follows:

(1) Winter NAO index had a overall increasing trend, except for the abrupt transitions during a decade from 1973 to 1982, when SST and CIL temperature followed generated echoes, that is, the trends changed correspondingly. The general decreasing trend of SST is opposite to the winter NAO index.
(2) Winter NAO index abrupt shift frequently may bring great changes on meteorological, physical and biogeochemical variables in the Black Sea. The variabilities in air temperature and wind caused by the winter NAO index influence SST and ventilation flux, and then affect oxygen, nitrate and phytoplankton. The ventilation flux from surface to CIL which led by wind variability changed the distributions of biogeochemical variables. After analysis on the results of the sensitivity experiments, the roles of meteorological forcing on affect oxygen, phytoplankton and nitrate from important to less important were air temperature, wind component U, then V, dew point temperature, and last sea level pressure.
(3) A performed model analysis can reveal a mechanism of reaction of the Black Sea biogeochemical regime on the decadal atmospheric variability. More intense ventilation should lead to an increase in both oxygen content in the CIL and supply of nutrient to the surface layer, which will potentially increase the biological productivity Therefore, the periods of increased concentrations of nitrate and phytoplankton should be correlated with the oxygen increase in the CIL, while the oxygen dynamics in the upper layer can be in a larger degree controlled by an interannual variability of the temperature.

The general response pattern of hydrophysical and biogeochemical variables in the Black Sea to NAO may be described as being mostly shaped by air temperature. However, taking into consideration the fact that most processes in the Black Sea are controlled by wind [25], one could expect that in 3D modelling framework wind will also have a pronounced impact. The fact that the results presented here do not fully support variations in temporal distribution of O_2 and H_2S derived from observations [6] could be due to the following problems: (1) in the present model, interannual changes in river runoff and eutrophication due to it has not been considered; (2) horizontal transport processes are also expected to play an important role. Therefore, the next step to do when simulating the long-term variability is to apply a 3D modelling framework.

Acknowledgements We would like to thank Dr. O. Podymov, Dr. J. Su and R. Kandilarov for their useful help. Atmospheric model data were produced by the European Centre for Medium-Range Weather Forecasts (ECMWF) and were kindly made available for the period 1958–2002 in the frame of SESAME project by the INGV, Italy. The study was funded by HYPOX project.

References

1. Spencer DW, Brewer PG (1971) Vertical advection diffusion and redox potentials as controls on the distribution of manganese and other trace metals dissolved in waters of the Black Sea. J Geophys Res 76:5877–5892
2. Shaffer G (1986) Phosphate pumps and shuttles in the Black Sea. Nature 321:515–517
3. Stanev EV, Staneva JV, Bullister JL, Murray JW (2004) Ventilation of the Black Sea Pycnocline. Parameterization of convection, numerical simulations and validations against observed chlorofluorocarbon data. Deep Sea Res 51(12):2137–2169
4. Murray JW, Codispoti LA, Friederich GE (1995) Oxidation-reduction environments: the suboxic zone in the Black Sea. Aquatic chemistry: interfacial and interspecies processes. Am Chem Soc Adv Chem Ser 244:157–176
5. Yakushev EV, Pollehne F, Jost G, Kuznetsov I, Schneider B, Urnlauf L (2007) Analysis of the water column oxic/anoxic interface in the Black and Baltic seas with a numerical model. Mar Chem 107:388–410
6. Konovalov SK, Murray JW (2002) Variations in the chemistry of the Black Sea on a time scale of decades (1960-1995). J Mar Syst 31:217–243
7. Oguz T (2005) Black sea ecosystem response to climatic teleconnections. Oceanography 18(2):122–133
8. Yakushev EV, Chasovnikov VK, Murray JW, Pakhomova SV, Podymov OI (2008) Vertical hydrochemical structure of the Black Sea. The Black Sea environment, The handbook of environmental chemistry, vol 5. Springer, Berlin, pp 277–307
9. Oguz T, Ducklow H, Malanotte-Rizzoli P, Murray JW (1998) Simulations of the Black Sea pelagic ecosystem by one-dimensional, vertically resolved, physical-biochemical models. Fish Oceanogr 7(3/4):300–304
10. Konovalov SK, Murray JW, Luther GW, Tebo BM (2006) Processes controlling the redox budget for oxic/anoxic water column of the Black Sea. Deep Sea Res II 53:1817–1841
11. Burchard H, Bolding K, Villareal MR (1999) GOTM, a general ocean turbulence model, theory, applications and test cases. European Commission Report EUR 18745 EN 103
12. Burchard H (2002) Applied turbulence modelling in marine waters. Lecture notes in earth sciences, vol 100. Springer, Berlin, p 229
13. Kondo J (1975) Air-sea bulk transfer coefficients in diabatic conditions. Bound Lay Meteor 9:91–112
14. Oguz T, Gilbert D (2007) Abrupt transitions of the top-down controlled Black Sea pelagic ecosystem during 1960-2000: evidence for regime-shifts under strong fishery and nutrient enrichment modulated by climate-induced variations. Deep Sea Res I. doi:10.1016/j.dsr.2006.09.010
15. Marshall FE, Cannizzo JK, Corbet RHD (1997) IAU Central Bureau for Astronomical Telegrams. Circular No. 6727. website: http://www.cfa.harvard.edu/iauc/06700/06727.html#Item1
16. Jones PD, Jonsson T, Wheeler D (1997) Extension to the North Atlantic oscillation using early instrumental pressure observations from Gibraltar and south-west Iceland. Int J Climatol 17:1433–1450

17. Murray JW, Stewart K, Kassakian S, Krynytzky M, Dijulio D (2005) Oxic, suboxic and anoxic conditions in the Black Sea. In: A. Gilbert, V. Yanko-Hombach and N. Panin (eds) Climate Change and Coastline Migration as Factors in Human Adaptation to the Circum-Pontic Region: From Past to Forecast. Kluwer Pub.
18. Yakushev EV, Debolskaya EI (2000) Particulate manganese as a main factor of oxidation of hydrogen sufide in redox zone of the Black Sea. IOC Workshop Report, vol 159. Kluwer Academic, Dordrecht, pp 592–597
19. Stanev EV, Peneva EL (2002) Regional sea level response to global climatic change: Black Sea examples. Glob Planet Change 32:33–47
20. Tsimplis MN, Josey SA, Rixen M, Stanev EV (2004) On the forcing of sea level in the Black Sea. J Geophys Res 109:C08015. doi:10.1029/2003JC002185
21. Staneva JV, Stanev EV (2002) Water mass formation in the Black Sea during 1991–1995. J Mar Syst 32:199–218
22. Tsimplis M, Zervakis V, Josey S, Peneva ES,Truglia MV, Stanev E, Lonello P, Malanotte-Rizzoli P, ArtaleV, Theocharis A, Tragou E, Oguz T (2006) Changes in the Oceanography of the Mediterranean Sea and their link to Climate Variability. In: Mediterranean Climate Variability, Lionello, Rizzoli and Boscolo (eds) Elsevier, Chapter 4, 217–272
23. Kazmin AS, Zatsepin AG, Kontoyiannis H (2010) Comparative analysis of the long-term variability of winter surface temperature in the Black and Aegean Seas during 1982–2004 associated with the large-scale atmospheric forcing. Int J Climatol 30:1349–1359
24. Belokopitov V (1998) Long-term variability of cold intermediate layer renewal conditions in the Black Sea. NATO TU-Black Sea Project Ecosystem Modelling as a Management Tool for the Black Sea, Symposium on Scientific Results. NATO ASI Series 2/47(2):47–52
25. Stanev EV, Bowman MJ, Peneva EL, Staneva JV (2003) Control of Black Sea intermediate water mass formation by dynamics and topography: comparisons of numerical simulations, survey and satellite data. J Mar Res 61:59–99
26. Rodi W (1987) Examples of calculation methods for flow and mixing in stratified fluids. J Geophys Res (C5), 92:5305–5328